

## $\alpha$ -Helical Hydrophobic Polypeptides Form Proton-Selective Channels in Lipid Bilayers

A. E. Oliver and D. W. Deamer

Section of Molecular and Cellular Biology, University of California-Davis, Davis, California 95616 USA

**ABSTRACT** Proton translocation is important in membrane-mediated processes such as ATP-dependent proton pumps, ATP synthesis, bacteriorhodopsin, and cytochrome oxidase function. The fundamental mechanism, however, is poorly understood. To test the theoretical possibility that bundles of hydrophobic  $\alpha$ -helices could provide a low energy pathway for ion translocation through the lipid bilayer, polyamino acids were incorporated into extruded liposomes and planar lipid membranes, and proton translocation was measured. Liposomes with incorporated long-chain poly-L-alanine or poly-L-leucine were found to have proton permeability coefficients 5 to 7 times greater than control liposomes, whereas short-chain polyamino acids had relatively little effect. Potassium permeability was not increased markedly by any of the polyamino acids tested. Analytical thin layer chromatography measurements of lipid content and a fluorescamine assay for amino acids showed that there were approximately 135 poly-leucine or 65 poly-alanine molecules associated with each liposome. Fourier transform infrared spectroscopy indicated that a major fraction of the long-chain hydrophobic peptides existed in an  $\alpha$ -helical conformation. Single-channel recording in both 0.1 N HCl and 0.1 M KCl was also used to determine whether proton-conducting channels formed in planar lipid membranes (phosphatidylcholine/phosphatidylethanolamine, 1:1). Poly-L-leucine and poly-L-alanine in HCl caused a 10- to 30-fold increase in frequency of conductive events compared to that seen in KCl or by the other polyamino acids in either solution. This finding correlates well with the liposome observations in which these two polyamino acids caused the largest increase in membrane proton permeability but had little effect on potassium permeability. Poly-L-leucine was considerably more conductive than poly-L-alanine due primarily to larger event amplitudes and, to a lesser extent, a higher event frequency. Poly-L-leucine caused two populations of conductive events, one in the 0.1–0.5 pA range, and one in the 1.0–5.0 pA range, whereas nearly all events caused by poly-L-alanine were in the 0.1–0.5 pA range at an applied voltage of +60 mV. The channel-like activity appeared to switch between conductive and nonconductive states, with most open-times in the range of 50–200 ms. We conclude that hydrophobic polyamino acids produce proton-conducting defects in lipid bilayers that may be used to model functional proton channels in biological membranes.

### INTRODUCTION

The movement of a charged particle through the low dielectric environment of a biological membrane is energetically unfavorable. Because many bioenergetic processes involve ion flux across membranes, ion channels are of fundamental importance to cell function. Considerable progress in this area has been made in recent years, yet the structural requirements for ion conductance across the lipid bilayer are not well understood.

In an effort to define a minimal lipid-peptide system that can support the channel-like transport of ions, we have investigated hydrophobic polyamino acids incorporated into lipid bilayers. Theoretical work on computer-generated models indicates that five or six hydrophobic transmembrane  $\alpha$ -helices, together in a bundle, should provide a low energy pathway through the bilayer for ion flux (Furois-Corbin and Pullman, 1986, 1987). Energy minimization profiles showed that at any axial level, ions can have a negative (favorable) interaction energy with the channel. It was suggested that

ions could move through the channel by hopping between carbonyl oxygens of peptide bonds, and that the presence of polar residues along the inner wall of the channel was not strictly necessary for ion conductance.

To our knowledge, this theoretical work has not been tested systematically in a physical system, in part because it is difficult to incorporate hydrophobic polyamino acids into lipid bilayers. In the research reported here, we investigated the effect of polyamino acids of different lengths and polarity on lipid bilayer permeability to protons and potassium ions. Both ions are physiologically important, and comparison of proton and potassium flux provided information about the conduction mechanism.

Due to the relative insolubility of the hydrophobic polyamino acids, a novel procedure for incorporating peptides into bilayers was developed. This procedure involves a brief incubation of a dried film containing lipid and polyamino acid at an elevated temperature, after which the lipid-polypeptide complex was prepared either as liposomes or as planar lipid membranes. The degree of polyamino acid association with the liposomes was determined by a sensitive fluorescence assay. FTIR spectroscopy was used to probe the secondary structure of peptides by comparison of the carbonyl-stretching (amide I) region (Byler and Susi, 1985, 1986, 1988; Byler et al., 1986; Susi and Byler, 1983). By this method, the percentage of total peptide existing in each secondary structure was determined.

Received for publication 15 September 1993 and in final form 17 February 1994.

Address reprint requests to Ann E. Oliver, Section of Molecular and Cellular Biology, Division of Biological Sciences, University of California-Davis, Davis, California 95616-8535. Tel.: 916-752-1094; Fax: 916-752-3085; E-mail: aeoliver@ucdavis.edu.

© 1994 by the Biophysical Society

0006-3495/94/05/1364/16 \$2.00

We found that approximately one hundred hydrophobic polyamino acids were associated with each liposome. Long-chain polyalanine and polyleucine caused substantial increases in proton permeability, whereas polyhistidine had little effect. Short-chain polyamino acids increased conductance as well, but markedly less than the long-chain compounds. Moreover, FTIR spectroscopy showed that, in a lipid environment, 66% of the long-chain polyalanine and 79% of the polyleucine exists in an  $\alpha$ -helical conformation. The observations with liposomes were confirmed by results from planar lipid membranes. That is, long-chain hydrophobic amino acids produced transient channel-like activity, highly selective for protons. Essentially no channel-like conductance was observed when potassium ions replaced hydrogen ions.

These observations suggest that protons are conducted by a specialized conductance mechanism, perhaps along hydrogen-bonded chains of water molecules similar to those permitting proton conduction through the gramicidin channel. The proton-selective defects have possible significance as a model for proton conductance through the  $F_0$  subunit of the ATP synthase in coupling membranes.

## MATERIALS AND METHODS

### Liposome preparation and polyamino acid incorporation

10 mg of 1-palmitoyl, 2-oleoyl-phosphatidylcholine (POPC)/phosphatidylglycerol (PG) (90:10) (Avanti Polar Lipids, Inc., Alabaster, AL) was evaporated from chloroform under a stream of  $N_2$  gas in a Corex test tube. For liposomes with incorporated polyamino acids, 1 mg of poly-L-alanine ( $M_r$  24,600), poly-L-leucine ( $M_r$  20,700), poly-L-histidine ( $M_r$  11,000) (all purchased from Sigma Chemical Co., St. Louis, MO), or a short form of poly-L-alanine ( $M_r$  4,900) (obtained from ICN Biochemicals, Cleveland, OH), was added to the dry lipid film, and both were dissolved in 50–100  $\mu$ l of trifluoroacetic acid (TFA). This combination was mixed gently by hand. The TFA was then evaporated from the mixture under a stream of  $N_2$  in a 60°C water bath for 30 min, leaving a film of peptide and lipid.

A heated incubation was conducted at this point. The tube was filled with argon to exclude oxygen, capped with Parafilm, then heated for variable time periods at three temperature ranges: 25, 50, or 100°C. After the incubation, 1 ml of 10 mM AMTT, which has a linear titration curve over the pH range 6–8, 10 mM ACES (*N*-[2-Acetamido]-2-aminoethanesulfonic acid), 10 mM MES (2-[*N*-Morpholino]-ethanesulfonic acid), 10 mM TES (*N*-tris-[hydroxymethyl]-methyl-2-aminoethanesulfonic acid), and 10 mM Tricine, all purchased from Sigma) with 0.1 M  $K_2SO_4$  and 0.5 mM pyranine (Eastman Kodak, Rochester, NY) at pH 7.4 were added to the polyamino acid/lipid film. The tube was again filled with argon and capped with Parafilm. This solution was bath-sonicated (Laboratory Supplies Co., Inc., Hicksville, NY) for 1 min to disperse the lipid, titrated to pH 7.4, then extruded 10–12 times through Nuclepore filters (Nuclepore Corp., Pleasanton, CA) under pressure with  $N_2$ . Larger pore diameter filters were used initially (1.0  $\mu$ m), followed by 0.6 and 0.2  $\mu$ m pore diameter filters.

The external dye was removed by passing the liposomes over a Sephadex G-50 column (Sigma) and replacing the external buffer with 10 mM AMTT with 0.1 M  $K_2SO_4$ , pH 7.4. Twice the original volume was collected off the column (2 ml), giving a lipid concentration of 5 mg/ml or 6.6 mM. Control liposomes were prepared in the same manner, except that no peptide was added to the dry lipid film before TFA dissolution.

### Measurement of proton flux ( $J_H$ ) and calculation of the proton permeability coefficient ( $P_H$ )

Pyranine fluorescence intensity, which has been shown to be a reliable measure of internal pH in liposomes (Kano and Fendler, 1978; Clement and Gould, 1981; Biegel and Gould, 1981), was used to measure hydrogen ion flux into phospholipid vesicles. In a magnetically stirred quartz cuvette, 1.5 ml of liposome dispersion (at 1.0 mM lipid) was monitored for pyranine fluorescence with an SLM 8000 spectrofluorometer (SLM Instruments, Inc., Urbana, IL) driven by an IBM PS 2/Model 30 computer. Excitation wavelength was set at 430 nm, and emission wavelength was set at 515 nm.

After a pH reading at time zero ( $t_0$ ), 1  $\mu$ l of 100  $\mu$ M valinomycin was added to the cuvette. The valinomycin provides a pathway for  $K^+$  counter ion movement, so a proton diffusion potential does not develop that would inhibit further proton flux. A slow time-based acquisition of pyranine fluorescence was taken over 5 min. After an initial baseline was obtained, acid was added to the cuvette in the form of 0.8945 M  $H_2SO_4$ , producing a pH jump in the external buffered solution (pH 7.4  $\rightarrow$  pH 6.4). A gradual fluorescence decrease over time was caused by proton leakage across liposome membranes and subsequent quenching of pyranine fluorescence.

To determine the initial pH gradient driving proton flux, 1  $\mu$ l of 100  $\mu$ M nigericin was added at 100 s to destroy any remaining proton gradient, and a second pH reading was taken when the fluorescence drop was complete. The pyranine fluorescence was then titrated back to the starting level with known volumes of 0.983 M NaOH. In addition, the internal to external volume ratio ( $V_i/V_o$ ) was determined by measuring the fluorescence of a known dilution of liposomes before and after the G-50 column.

From the slope of the line caused by proton flux, the concentration of lipid in the cuvette, and the ratio of internal to external volume, proton flux was calculated as shown in Eq. 1.

$$J_H = \frac{(\text{mol } H^+)(V_i/V_o)}{\text{area of lipid } (cm^2) (s)} \quad (1)$$

The proton permeability coefficient was then calculated (Nichols and Deamer, 1980; Perkins and Cafiso, 1986) as follows.

$$P_H = \frac{J_H (\text{mol } H^+ \text{ cm}^{-2} \text{ s}^{-1})}{H^+ \text{ gradient } (\text{mol } H^+ \text{ cm}^{-3})} \quad (2)$$

It should be noted here that because of special properties of the proton transport mechanism,  $P_H$  can only be used to compare membrane permeabilities to protons at the same pH value (Deamer and Nichols, 1989). The definition we use here also assumes that only protons contribute to the decay of pH gradients, and not hydroxide ions.

### Measurement of potassium flux ( $J_K$ ) and calculation of the potassium permeability coefficient ( $P_K$ )

Liposomes were prepared as described above except that internal buffer was 10 mM AMTT and 0.2 M  $K_2SO_4$  at pH 7.5 with no dye present. 200- $\mu$ l aliquots of liposomes were put over a Sephadex G-50 column, replacing the external buffer with  $K^+$ -free buffer (10 mM AMTT with 0.3 M choline chloride at pH 7.5). A potassium-selective electrode was used to measure  $K^+$  efflux from liposomes, and flux  $J_K$  was defined as

$$J_K = \text{mol } K^+ \text{ cm}^{-2} \text{ s}^{-1}. \quad (3)$$

Dividing the value for flux by the potassium gradient ( $4 \times 10^{-4}$  mol  $cm^{-3}$ ) gives the potassium permeability coefficient.

$$P_K = \frac{J_K}{K^+ \text{ gradient}} \quad (4)$$

### Determination of the polyamino acid:liposome ratio

Liposomes were prepared as previously described, except that distilled water was used as both internal and external media and that the column was

composed of a Sepharose 4B-200 gel. This gel removed unincorporated polyamino acids, such that only liposome-associated peptides were collected from the column. The 2 ml of liposomes collected from the column was divided into four 0.5-ml aliquots. One aliquot was saved for lipid extraction. The three remaining aliquots were placed in separate 1.5 ml septum vials. HCl was added to each vial (0.5 ml, 12 N), bringing the HCl concentration to 6 N. The vials were filled with argon and heated in a Temp-Blok Module Heater (American Scientific Products, McGaw Park, IL) to 110°C for 24 h to hydrolyze the polyamino acids.

After the peptide hydrolysis, the HCl was evaporated under a stream of N<sub>2</sub>. A dry residue, composed primarily of the hydrolysis products, amino acids, and fatty acids, remained. Two washes, the first with acetone (100  $\mu$ l), and the second with distilled water (0.5 ml), were used to dissolve the residue in each vial. Both washes were transferred to a clean borosilicate test tube. A fluorescamine assay for primary amines was used to quantify the amino acids. Sodium borate (1.0 ml, 200 mM, pH 9) was added to each sample. Each tube was checked with a Fisher Accumet pH meter to be at pH 9, then while vortexing, fluorescamine (0.5 ml, 5 mg/ml in acetone; Sigma) was added to each tube. The fluorescamine fluorescence was measured on the SLM 8000 spectrofluorometer (excitation 390 nm, emission 480 nm), and matched against a standard curve for amino acid concentration.

The unhydrolyzed aliquot collected from the 4B-200 column was extracted with 1.2 ml of CHCl<sub>3</sub>: MeOH (2:1). After initial vortexing, KCl was added to bring the aqueous concentration to 1 M. Each tube was then re-vortexed, placed on ice for 1 min, and centrifuged for 1 min at 850  $\times$  g.

An Iatroscan TH-10 flame ionization detector (Iatron Laboratories, Tokyo, Japan) was used to analyze the extracted lipids, which were spotted from chloroform solutions onto Iatroscan rods, then developed in CHCl<sub>3</sub>/MeOH/H<sub>2</sub>O (65:25:4) with 1% v/v acetic acid. When the solvent front approached the top of the rods, the rods were removed and placed in a drying oven for 10–15 min. The rods were then subjected to hydrogen flame ionization detection linked to a chart recorder. The area under the peaks was matched against a standard curve to quantify the lipid. Assuming a vesicle diameter of 0.2  $\mu$ m (400,000 lipids per liposome), a simple calculation, using the data from the fluorescamine assay and the analytical thin layer chromatography gives the ratio of polyamino acid molecules per liposome.

## Fourier transform infrared spectroscopy

Fourier transform infrared (FTIR) spectroscopy was performed on polyamino acids and lipids dried to a film from TFA. Polyamino acid (1 mg) and lipid (2 mg POPC/PG (90:10)) were dissolved in 50  $\mu$ l of TFA. The TFA solution was then placed on a CaF crystal and dried to a film under a stream of N<sub>2</sub>. The dried film was deuterated by placing it in a D<sub>2</sub>O-saturated atmosphere for 18 h. The sample was placed between CaF crystals inside a Perkin Elmer 1750 optical bench flushed with dry N<sub>2</sub>, and analyzed with an IBM PS/DOS computer. Background of the system and CaF crystals was taken and subsequently subtracted from the sample spectra. 50 interferograms in the range 4000–1000 cm<sup>-1</sup> were averaged for each spectrum. A spectrum of a pure lipid film (2 mg of POPC/PG (90:10) dried from 50  $\mu$ l of TFA) was taken and subtracted from the polyamino acid/lipid spectra. The resulting difference spectra represent the polyamino acids in a lipid environment, but do not include any of the lipid peaks. Second derivatives were taken of the difference spectra and analyzed for positions and relative intensities of the component peaks of the amide I region (1700–1620 cm<sup>-1</sup>) for each peptide (Byler and Susi, 1986, 1988; Susi and Byler, 1983).

Once the positions of the component peaks of the amide I band were determined from the second derivative spectrum, the program Lab Calc (Galactic Industries Corp.) was used to deconvolve the original spectrum in the amide I region. Areas under the component peaks were integrated, and their percentage of the total peak was calculated. By this method, the percentage of the total membrane-embedded peptide existing in each secondary structure was obtained.

## Preparation of bilayer cups

Conical polystyrene sample cups were purchased from Fisher Scientific (Pittsburgh, PA), and a single 0.5-mm aperture was hand-drilled into each

cup. The cups were washed in commercial detergent and subsequently tumbled for 30 min in distilled water. Each cup was then rinsed 3 times in nanopure water and once in HPLC grade methanol (Fisher).

The aperture was pretreated with 1  $\mu$ l of a solution containing 30 mg/ml each of L- $\alpha$ -phosphatidylethanolamine (egg) and L- $\alpha$ -phosphatidylserine (brain-sodium salt) in decane (Aldrich Chemical Co., Inc., Milwaukee, WI), and allowed to air dry. Both phospholipids were purchased from Avanti and used without further purification.

## Preparation of membrane-forming solution

Small glass test tubes were washed in 1 M nitric acid and rinsed in nanopure water and methanol. Into each test tube, 1.25 mg of L- $\alpha$ -phosphatidylethanolamine (PE) and 1.25 mg of L- $\alpha$ -phosphatidylserine (PS) were added and the chloroform evaporated under a stream of nitrogen. The lipid film was placed under a vacuum for 30 min to remove any remaining chloroform. To the lipid film was added 1.0 mg of poly-L-alanine (*M*<sub>r</sub> 24,600 or 4,900), poly-L-leucine (*M*<sub>r</sub> 20,700), poly-L-histidine (*M*<sub>r</sub> 10,800), or nothing in the case of the controls. All polyamino acids were purchased from Sigma, except for poly-L-alanine (*M*<sub>r</sub> 4,900) which was obtained from ICN Biochemicals (Cleveland, OH).

The lipid and peptide were codissolved in 50  $\mu$ l of TFA (Sigma). The tube was subsequently placed in a water bath at 60°C, and the TFA was removed by evaporation under a stream of nitrogen. This dried peptide and lipid film was subjected to a heated incubation of 1 min at 100°C. After the incubation, 50  $\mu$ l of hexadecane (Aldrich) was added to the peptide and lipid film. This hexadecane solution was also heated for 1 min at 100°C, and was bath sonicated for 1 min to force as much peptide into solution with the lipid as possible. The final lipid concentration was 30 mg/ml each of PE and PS. The membrane-forming solutions for control membranes were prepared in the same way, except that no peptide was added.

The membrane-forming solutions containing gramicidin D were also prepared in the same manner, except that the TFA dissolution and heated incubation steps were omitted. Gramicidin D (ICN Biochemicals) was used both as an indicator of bilayer structure and as a comparison for the conductive events caused by the long-chain hydrophobic polyamino acids. It was included at a peptide/lipid ratio of 1:10<sup>6</sup>.

## Experimental set-up

A double-bored teflon chamber was soaked overnight in 50% nitric acid, and subsequently rinsed in distilled water, nanopure water, and methanol. A pretreated polystyrene membrane cup was fit securely into one side of the chamber, leaving the drilled aperture as the only pathway between the two buffer wells. Buffer wells were filled with identical solutions.

A reference electrode was placed in the *cis*-buffer well, and the head stage electrode was placed in the *trans*-buffer well. A Dagan 3900 Integrating Patch Clamp was used in the voltage clamp mode to apply a specified potential and measure ionic current across the planar bilayer. A Four Pole Low Pass Bessel Filter was in line and filtering at 20 Hz. The current was monitored with a Tektronix 5113 dual beam storage oscilloscope and recorded with a Fisher Scientific Recordall Series chart recorder. A large Faraday cage housed the planar membrane apparatus, and the Faraday cage sat on a marble table supported by rubber pillows to decrease the detectable noise level.

## Experimental procedure

The buffer wells were both filled with either filtered 0.1 N HCl or filtered 0.1 M KCl plus 10 mM MES (all from Sigma) at pH 6.5. During a 10 mV square wave, membranes were painted across the aperture according to the method of Mueller et al. (1962, 1963), after which a 100 mV square wave was applied for 1 min to stabilize the membrane. Recordings were taken at applied voltages of +60, +100, and +200 mV for each membrane. At least four membranes were sampled for each combination of peptide and buffer.

## Data analysis

For all combinations of peptides and buffers at +60 mV, mean amplitudes and frequencies are presented. Data for duration of open times are presented as a range of values rather than as averaged points, because it was not always clear (e.g., for gramicidin) which channel closure corresponded to which channel opening. The frequency ratio was also calculated for each peptide buffer combination as

$$\text{Ratio} = \frac{\text{Mean frequency of events for membranes containing peptide in solution X}}{\text{Mean frequency of events for control membranes in solution X}}$$

In addition, for the two conductive polyamino acids (polyleucine and long-chain polyalanine in HCl), the current/voltage relations are compared to those for gramicidin. Finally, histograms of amplitude and duration of open times provide information regarding the distribution of these data at various applied voltages.

## RESULTS

### Polyamino acids are incorporated into liposomes during heated incubation of a polyamino acid/lipid film

In preliminary experiments, the temperature and length of the lipid-peptide incubation period were varied, and the effects on the proton permeability coefficient of the resulting liposome membranes were determined. Fig. 1 shows the ratio of the mean experimental proton permeability coefficient to the mean control proton permeability coefficient ( $P_{ex}/P_c$ ) as a function of incubation length for three temperature ranges.

A temperature of 100°C was most effective, but although there was some variability, the length of incubation did not seem to be critical. Even with a 10-s incubation at 100°C, polyalanine was able to cause a fivefold increase in the  $P_H$  when compared to control liposomes. The 100°C incubation did not damage the lipid or cause the formation of any breakdown products as measured by analytical thin layer chromatography of lipid extracted after a 30 min, 100°C incubation (data not shown).

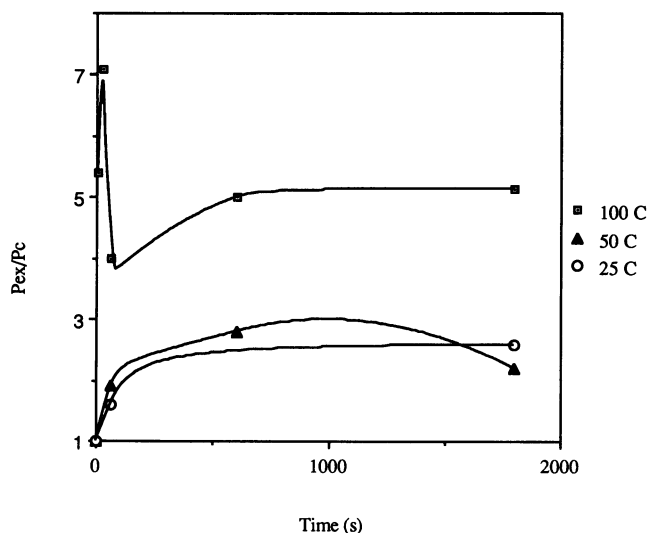


FIGURE 1 Mean ratio of  $P_{ex}/P_c$  for long-chain polyalanine when subjected to heated incubations of different lengths and temperatures.

### Both alamethicin and long-chain hydrophobic polyamino acids caused marked increases in proton permeability

Liposomes with polyamino acids were prepared using a 30 min, 100°C heated incubation. Fig. 2 compares  $P_{ex}/P_c$  for various polyamino acids. The mean ratio of  $P_{ex}/P_c$  for long-chain polyalanine was 5.2 ( $n = 2$ ), and for polyleucine it was 6.3 ( $n = 3$ ). These are in the range seen with alamethicin (ALA), a known channel-forming protein (Eisenberg et al., 1973; Hall et al., 1984). When alamethicin was added externally to liposomes at a ratio of 100 molecules per liposome, it caused a mean sevenfold increase in the proton permeability coefficient ( $n = 2$ ). Polyhistidine did not increase the proton permeability above control values ( $n = 3$ ).

Potassium permeabilities are also compared in Fig. 2. In contrast to the result obtained for proton permeability, the mean ratio of experimental permeability coefficient to control permeability coefficient for potassium was less affected by the hydrophobic polyamino acids. Using a heated incubation of 1 min at 100°C, the mean ratio of  $P_{ex}/P_c$  for long-chain polyalanine and polyleucine were 2.4 ( $n = 6$ ) and 1.6 ( $n = 5$ ) respectively. Under the same preparation conditions, polyhistidine also seemed to have a minor effect, with a mean  $P_{ex}/P_c$  of 1.8 ( $n = 4$ ).

### Long-chain polyalanine caused a greater proton permeability increase than short-chain polyalanine

To determine what effect the length of the peptide has on its ability to increase membrane permeability, two different molecular weights of polyalanine (24,600 and 4,900) were compared for their effect on  $P_H$  (see Fig. 3). A heated incubation of 1 min at 100°C was used during liposome formation. Poly-L-alanine ( $M_r$  24,600), which has approximately 275 residues

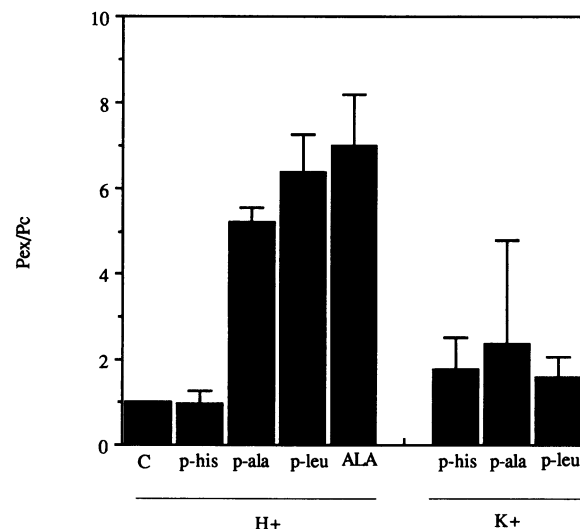


FIGURE 2 Mean ratios of  $P_{ex}/P_c$  for different polyamino acids with regard to proton and potassium permeability coefficients of liposome membranes.

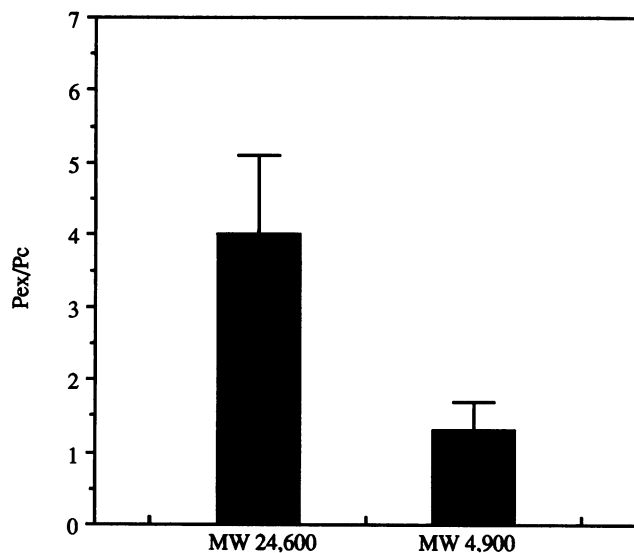


FIGURE 3 Mean ratios of  $P_{ex}/P_c$  for polyalanine  $M_r$  24,600 and 4,900 with regard to proton permeability coefficients of liposome membranes.

per peptide, had a mean  $P_{ex}/P_c$  ratio of 4.0 ( $n = 3$ ), whereas, poly-L-alanine ( $M_r$  4,900), with approximately 55 residues per peptide had a mean  $P_{ex}/P_c$  ratio of only 1.3 ( $n = 3$ ).

Furthermore, as shown in Table 1, measurements of the polyamino acid/lipid ratios indicated that, although long-chain polyalanine had a more pronounced proton-conducting effect, there were actually fewer molecules associated with each liposome than was the case for the short-chain polyalanine. Long-chain polyalanine and polyleucine had peptide/lipid ratios of 1:6150 and 1:2960, respectively. These peptide to lipid ratios correspond to approximately 65 molecules per liposome for long-chain polyalanine, and 135 molecules per liposome for polyleucine. Short-chain polyalanine, which had a peptide/lipid ratio of 1:1450, associated at the level of 275 molecules per liposome. Thus, although short-chain polyalanine is lipophilic and associates with liposomes in larger numbers, it was less able to form ion-conducting defects than long-chain polyalanine.

Polyhistidine also associated with the liposomes to a certain extent. The peptide/lipid ratio for polyhistidine was 1:2000, which corresponds to approximately 200 molecules of polyhistidine per liposome. Thus, it is clear that the lack of increase in proton permeability caused by polyhistidine was not due to its absence from the liposomes, but rather its inability to mediate proton conduction through the membrane.

TABLE 1 Polyamino acid:lipid and polyamino acid:liposome ratios

Polyamino acid	$N$	Peptide:lipid ratio	Approximate number of molecules/liposome
s/c polyalanine	6	1:1450	275
l/c polyalanine	6	1:6150	65
polyleucine	6	1:2960	135
polyhistidine	6	1:2000	200

### Long-chain hydrophobic polyamino acids form $\alpha$ -helices in a lipid environment

Because this investigation is based on the theoretical possibility (Furois-Corbin and Pullman, 1986, 1987) that bundles of hydrophobic  $\alpha$ -helices could conduct ions across a membrane, it was important to determine the conformation of the polyamino acids in a lipid environment. FTIR spectroscopy was used to probe the secondary structure of the peptides by a comparison of the carbonyl stretching (amide I) band at 1700–1620  $\text{cm}^{-1}$ . Each polyamino acid (1 mg) was dried to a film with 2 mg of POPC/PG (90:10) out of TFA onto CaF crystals, and saturated in a  $\text{D}_2\text{O}$  atmosphere for 18 h. FTIR difference spectra from each polyamino acid/lipid film and a  $\text{D}_2\text{O}$ -saturated pure lipid film are shown in Fig. 4. Also shown are the second derivatives of each difference spectrum. Table 2 provides assignments of secondary structure for wave number positions within the amide I band.

For both long-chain polyalanine and polyleucine, the  $\alpha$ -helical peak predominates. As seen in Fig. 4 *a*, the second derivative spectrum for polyleucine shows only one main peak (peak 1, 1656  $\text{cm}^{-1}$ ) in the  $\alpha$ -helical position. The second derivative spectrum for long-chain polyalanine, shown in Fig. 4 *b*, also has its major peak in the  $\alpha$ -helical position (peak 2, 1657  $\text{cm}^{-1}$ ). There are also minor peaks in the extended chain (peak 1, 1630  $\text{cm}^{-1}$ ) and turns positions (peak 3, 1669  $\text{cm}^{-1}$ ).

For polyhistidine and short-chain polyalanine, however, there was a broader distribution among component peaks of the amide I band. The polyhistidine second derivative spectrum (Fig. 4 *c*) showed a high degree of extended chain (peak 1, 1627  $\text{cm}^{-1}$ ; peak 4, 1673  $\text{cm}^{-1}$ ) with a minor contribution of unordered (peak 2, 1648  $\text{cm}^{-1}$ ) and  $\alpha$ -helix (peak 3, 1655  $\text{cm}^{-1}$ ). The secondary structure of short-chain polyalanine (Fig. 4 *d*) was distributed between extended chain (peak 1, 1628  $\text{cm}^{-1}$ ; peak 2, 1638  $\text{cm}^{-1}$ ), disordered (peak 3, 1647  $\text{cm}^{-1}$ ),  $\alpha$ -helix (peak 4, 1656  $\text{cm}^{-1}$ ), and turns (peak 5, 1662  $\text{cm}^{-1}$ ; peak 6, 1683  $\text{cm}^{-1}$ ).

Once the positions of the component peaks are found from the second derivative spectra, deconvolution of the amide I band using the program Lab Calc provides an estimate of the percentages contributed by each component peak to the total peak. Using this method, the percentage of total peptide existing in each secondary structure was obtained.

Fig. 5 shows histograms illustrating the percentage of amide I band contributed by the structural conformations of turns,  $\alpha$ -helix, random coil and extended chain. Long-chain polyalanine and polyleucine were predominantly  $\alpha$ -helical in the membrane environment. Long-chain polyalanine (Fig. 5 *a*) was 66%  $\alpha$ -helix in nature and polyleucine (Fig. 5 *b*) had a 79% contribution of  $\alpha$ -helical secondary structure.

In contrast, short-chain polyalanine (Fig. 5 *c*) was split between  $\alpha$ -helix and extended chain with a 43% contribution from both. Polyhistidine (Fig. 5 *d*) was almost entirely extended chain, showing an 87% contribution from this

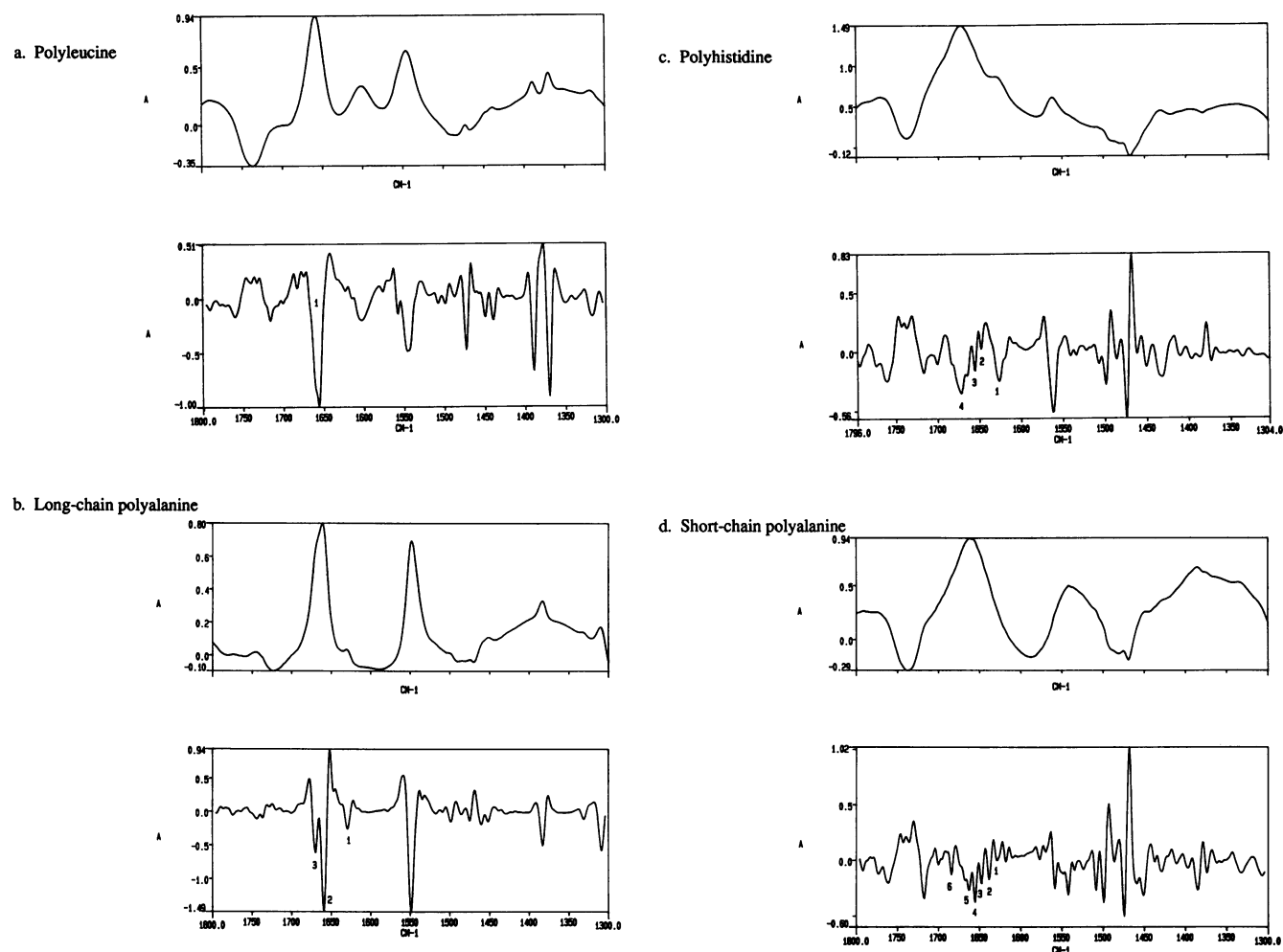


FIGURE 4 FTIR difference spectra and second derivative spectra in the region of the protein amide I band. Polyamino acid (1 mg) was dried to a film with lipid (2 mg of POPC/PG (90:10)) onto CaF crystals. Difference spectra were taken between the polyamino acid/lipid films and a pure lipid film. Component peaks of the amide I band are labeled in the second derivative spectra: (a) polyleucine; (b) long-chain polyalanine; (c) polyhistidine; (d) short-chain polyalanine.

TABLE 2 FTIR wavenumber assignments

Wave-number (cm <sup>-1</sup> )	Assignment	Reference
1624 ± 4	extended chain	Byler et al., 1986; Byler and Susi, 1985
1631 ± 3	extended chain	Byler et al., 1986; Byler and Susi, 1985
1637 ± 3	extended chain	Byler et al., 1986; Byler and Susi, 1985
1645 ± 4	unordered	Byler et al., 1986; Byler and Susi, 1985
1650–1660	α-helix	Braiman and Rothschild, 1988
1653 ± 4	α-helix	Byler et al., 1986; Byler and Susi, 1985
1663 ± 4	turns	Byler et al., 1986; Byler and Susi, 1985
1671 ± 3	turns	Byler et al., 1986; Byler and Susi, 1985
1675 ± 5	extended chain	Byler et al., 1986; Byler and Susi, 1985
1680 ± 2	turns	Byler et al., 1986; Byler and Susi, 1985
1689 ± 2	turns	Byler et al., 1986; Byler and Susi, 1985
1694 ± 2	turns	Byler et al., 1986; Byler and Susi, 1985

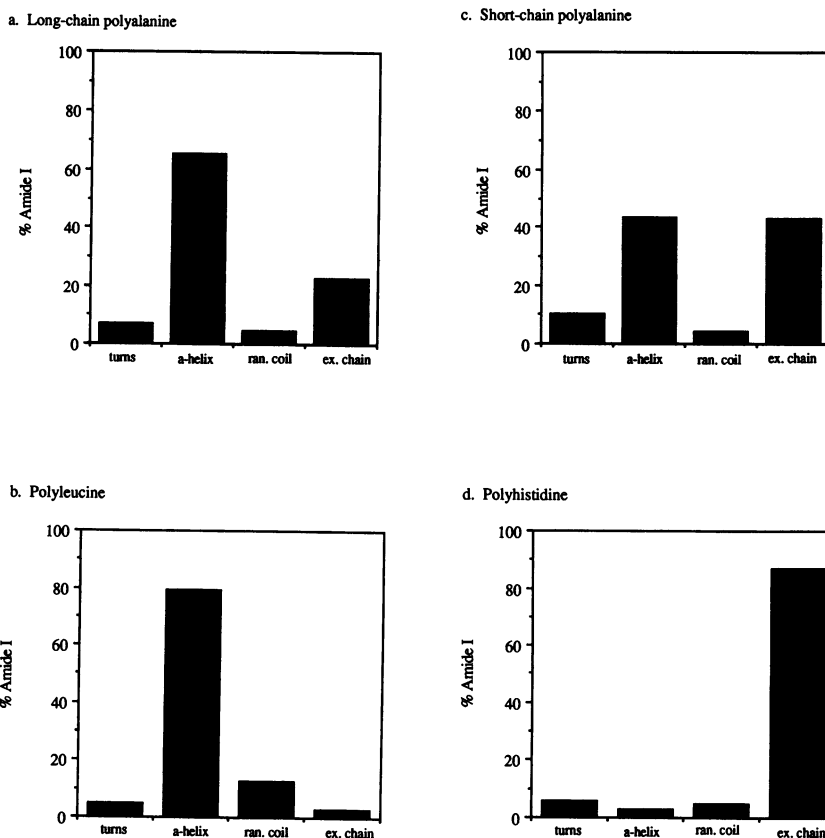
structural conformation. It is important to note that all of the above values are measured in films of mixed lipid-peptide hydrated with D<sub>2</sub>O. We have no direct evidence that similar proportions of α-helix and other conformations exist in the bilayer structures of liposomes and planar membranes.

### Long-chain hydrophobic polyamino acids in HCl produce current fluctuations in planar bilayers

Recordings were taken from control membranes with no peptide present as well as from membranes doped with long-chain (l/c) or short-chain (s/c) polyalanine, polyleucine, polyhistidine, or gramicidin D. A sample trace from each type of membrane in 0.1 N HCl and 0.1 M KCl is shown in Fig. 6. The presence of characteristic channels in the gramicidin traces (Fig. 6, *a* and *b*) indicates a true bilayer structure for the membranes. Mean gramicidin conductances were 48 pS in HCl and 15 pS in KCl.

The sample size, mean amplitude, mean frequency, and range of duration are given in Table 3 for the conductive events caused by each peptide tested in both 0.1 N HCl and 0.1 M KCl at an applied potential of +60 mV. Long-chain polyalanine and polyleucine were the only polyamino acids to cause a significant level of conductive activity, and they did so only in the HCl media. Polyleucine, in fact, caused many more conductance events of much larger amplitude

FIGURE 5 Histograms showing percent of polyamino acids in  $D_2O$ -saturated peptide/lipid films to exist in each secondary structural conformation. Each polyamino acid was dried to a film with POPC/PG (90:10) from TFA, then deuterated in a  $D_2O$ -saturated atmosphere for 18 h. The difference spectra, specifically in the amide I region, between a peptide/lipid film and a pure lipid film was deconvolved using Lab Calc to find percent contributions of each component peak to the total amide I band. (a) long-chain polyalanine; (b) polyisoleucine; (c) short-chain polyalanine; (d) polyhistidine.



than did long-chain polyalanine. Short-chain polyalanine and polyhistidine caused very little conductive activity either in HCl or KCl. The frequency of current fluctuations in these membranes was not significantly higher than the random noise seen in the control membranes.

#### Event frequency is most affected by polyisoleucine

The most striking result seen in Table 3 is that polyisoleucine causes conductive events in HCl close in amplitude, duration, and frequency to those produced by gramicidin. In fact, the most significant difference between the conductive polyamino acid membranes (1/c polyalanine and polyisoleucine in HCl) and the others is seen in the frequency of current fluctuations.

Except for the large mean amplitude of the events caused by polyisoleucine in HCl, all the values for mean amplitude and duration of open times fall in the same range of 0.1–0.5 pA of current and open times ranging from 50 ms to several seconds. The mean frequencies of events caused by long-chain polyalanine and polyisoleucine in HCl, however, are 27.4 events/min and 76.0 events/min, respectively. These values are 10 to 30 times higher than those seen for the less conductive membranes.

To compare better the frequency of current fluctuations in membranes doped with polyamino acids to control membranes, frequency ratios were calculated. The frequency of events for polyamino acid membranes was divided by the frequency of events for control membranes in the same so-

lution. Table 4 provides the frequency ratios for membranes containing each of the polyamino acids studied in both HCl and KCl.

As seen in Table 4, long-chain polyalanine and polyisoleucine caused 50- and 150-fold increases, respectively, in the frequency of current fluctuations over control membranes. This increase in event frequency above the level seen in control membranes far exceeds that caused by any other polyamino acid. Thus, the frequency of current fluctuations seems to be the parameter of conductivity most affected by the presence of polyamino acids, and the long-chain hydrophobic polyamino acids have the greatest effect on this parameter, specifically in 0.1 N HCl.

#### I/V curves for gramicidin, polyisoleucine, and polyalanine are not voltage-dependent

Current/voltage relations were constructed for gramicidin in HCl and KCl, and for polyisoleucine and long-chain polyalanine in HCl. As shown in Fig. 7a, gramicidin displays ohmic (linear) conductance in both 0.1 N HCl and 0.1 M KCl, indicating a lack of voltage dependence of the channel for ionic conduction. The slope of the I/V curve for gramicidin in HCl is approximately three times that in KCl. This illustrates the greater conductance of protons through the gramicidin pore compared to that of potassium ions, as has been noted by other investigators (Myers and Haydon, 1972; Levitt et al., 1985; Deamer and Nichols, 1989).

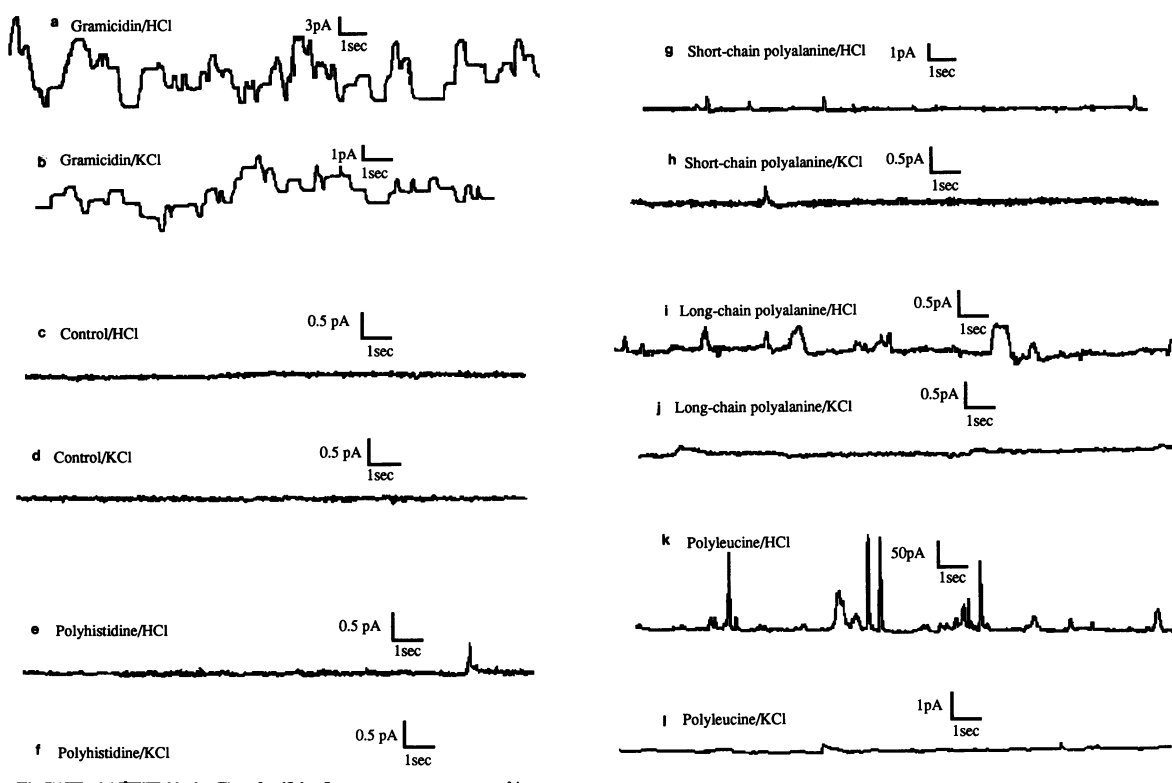


FIGURE 6 Sample traces from PE/PS (1:1) planar bilayers at +60 mV applied potential taken from recordings in either 0.1 N HCl or 0.1 M KCl. The membranes were formed in the presence of the following peptides: (a) gramicidin D in HCl; (b) gramicidin D in KCl; (c) no peptide (control) in HCl; (d) no peptide (control) in KCl; (e) polyhistidine in HCl; (f) polyhistidine in KCl; (g) short-chain polyalanine in HCl; (h) short-chain polyalanine in KCl; (i) long-chain polyalanine in HCl; (j) long-chain polyalanine in KCl; (k) polyleucine in HCl; and (l) polyleucine in KCl. Images were computer-generated by scanning data from chart records.

TABLE 3 Conductivity parameters for planar bilayers at +60 mV

Peptide	Buffer	<i>N</i>	$\bar{x}I$ (pA)	Frequency (events/min)	Range of duration (ms)
Control	HCl	3	0.5	0.5	50–1000
Control	KCl	6	0.5	1.4	30–200
Gram	HCl	500	2.8	159.7	50–6000
Gram	KCl	613	0.9	87.4	50–4000
p-leu	HCl	399	3.4	76.0	50–10000
p-leu	KCl	3	0.4	1.5	100–300
l/c p-ala	HCl	516	0.4	27.4	20–2000
l/c p-ala	KCl	33	0.4	2.1	50–6000
s/c p-ala	HCl	32	0.4	2.0	50–500
s/c p-ala	KCl	17	0.2	1.3	50–300
p-his	HCl	11	0.4	1.5	50–1000
p-his	KCl	8	0.2	1.1	50–5500

The current/voltage relations for polyleucine and long-chain polyalanine in 0.1 N HCl are shown in Fig. 7 *b*. The steepness of the I/V curve for polyleucine compared to that of long-chain polyalanine is striking. The slope of the polyleucine curve is approximately 60 times that for long-chain polyalanine. Both curves display mostly ohmic conductance, except for a slight bend in the polyleucine curve between 0 and +60 mV applied potential. Linear I/V curves were expected for the polyamino acid induced defects, due to the unlikelihood that bundles of purely hydrophobic  $\alpha$ -helices could open and close in a voltage-dependent man-

TABLE 4 Frequency ratios

Peptide	Frequency Ratio in HCl	Frequency Ratio in KCl
p-leu	152.0	1.1
l/c p-ala	54.8	1.5
s/c p-ala	4.0	0.9
p-his	2.8	0.8

ner. It is more likely that when defects in the membrane do occur, more protons are conducted at higher applied voltages.

#### Amplitude distribution of conductive events

Histograms of amplitude or open time duration can give more information than simple arithmetic means, because they can indicate separate populations of conductive events. For this reason, amplitude histograms were constructed for the conductive membranes: gramicidin in HCl and KCl, and long-chain polyalanine and polyleucine in HCl. Histograms are presented on a semilog scale due to the wide distribution of amplitude size.

As shown in Fig. 8, at an applied voltage of +60 mV, the amplitudes of gramicidin channels in HCl (Fig. 8 *a*) vary over a wider range than gramicidin channels in KCl (Fig. 8 *b*). In HCl, the most common amplitude is 2 pA, and



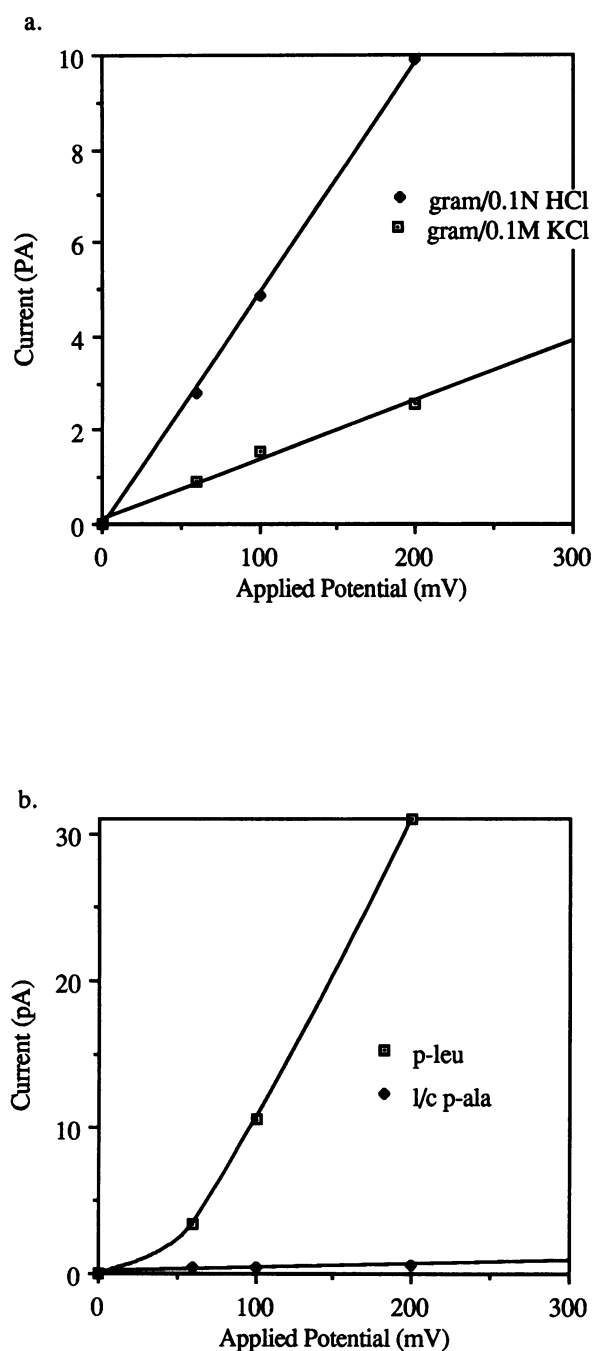
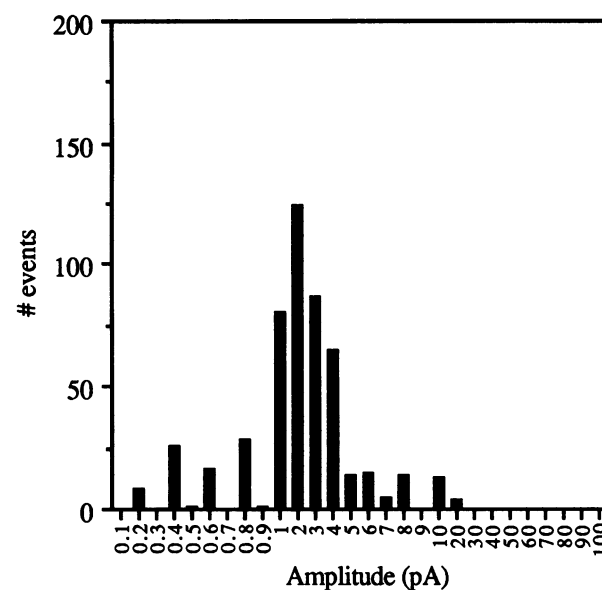


FIGURE 7 Current/voltage relations of current fluctuations produced by three peptides incorporated into PE/PS (1:1) planar bilayers. (a) gramicidin D channels in 0.1 N HCl and 0.1 M KCl; and (b) polyleucine and long-chain polyalanine-induced defects in 0.1 N HCl.

the data points fall in a roughly bell-shaped distribution. In KCl, on the other hand, event amplitudes are grouped tighter toward the lower end of the scale, with the most common amplitude being 1 pA.

The amplitude histogram for membranes doped with long-chain polyalanine in HCl at an applied potential of +60 mV is shown in Fig. 9. The most common amplitude was 0.1 pA, with the number of occurrences falling exponentially as amplitude increases. As was the case for the gramicidin chan-

a. Gramicidin/HCl



b. Gramicidin/KCl

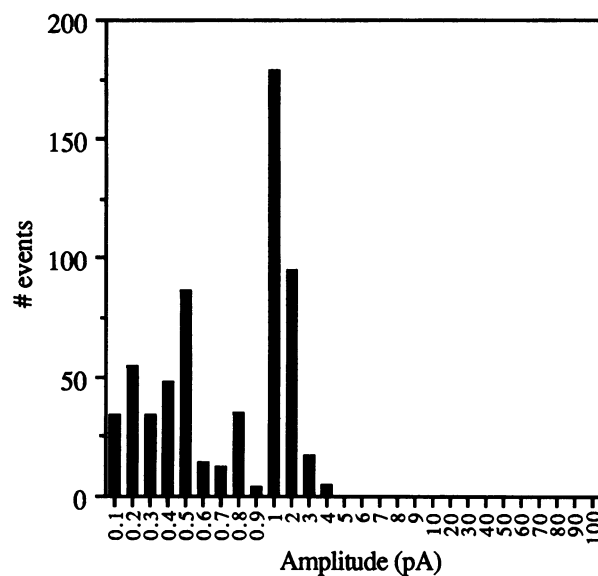


FIGURE 8 Amplitude histograms for gramicidin D channels in PE/PS (1:1) planar bilayers at +60 mV applied potential (a) in 0.1 N HCl, and (b) in 0.1 M KCl.

nels, the polyalanine-induced defects generally fall within a single population of events.

Amplitudes of the polyleucine-induced defects, however, had a much wider distribution. Fig. 10 displays the amplitude histograms for polyleucine membranes in HCl at applied voltages of +60, +100, and +200 mV. At an applied voltage of +60 mV (Fig. 10 a), there are two populations of amplitudes evident, one in the range 0.1–0.5 pA, and one in the

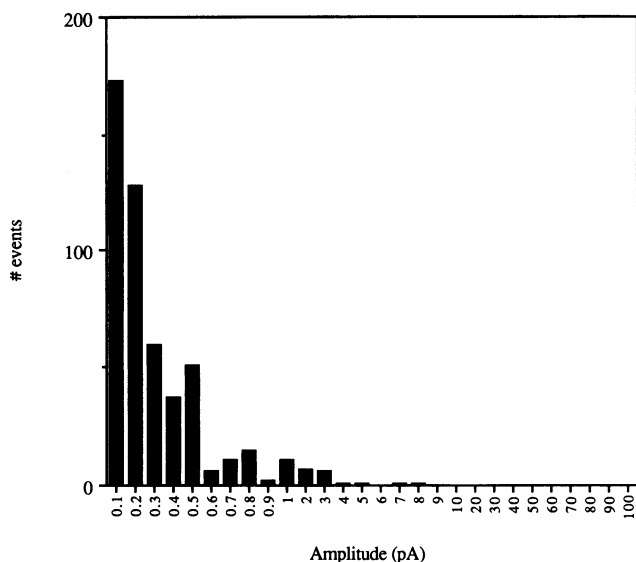


FIGURE 9 Amplitude histogram for long-chain polyalanine-induced defects in PE/PS (1:1) planar bilayers at +60 mV applied potential in 0.1 N HCl.

range 1.0–5.0 pA. As the applied potential was increased to +100 mV (Fig. 10 *b*), the higher amplitude population predominated, and several events were also seen at the much larger amplitudes of 50–200 pA. Finally, at an applied potential of +200 mV (Fig. 10 *c*), the population of events at 1.0–5.0 pA again diminished as the distribution became delocalized, and many events appeared in the 100–800 pA range.

### Open time distribution of conductive events

Histograms of open time duration provide information regarding the distribution of data that is unavailable from a simple mean. Because most events caused by polyleucine and long-chain polyalanine were wide spikes in shape, it was fairly clear which event opening corresponded to which closing. Thus, it was possible to construct open time duration histograms for the conductive membranes of long-chain polyalanine and polyleucine in HCl. As was the case for the amplitude histograms, a semilog scale is used for the duration histograms, due to the wide distribution of open times.

Fig. 11 shows the open time duration histogram for long-chain polyalanine membranes at the applied voltage of +60 mV. A large majority of the open times ranged from 50 to 500 ms, but there was also a small population of longer-lived events in the range 0.9–2.0 s.

The effect on open time duration of increasing the applied voltage was studied in polyleucine membranes, and is illustrated in Fig. 12. At an applied voltage of +60 mV (Fig. 12 *a*), nearly all open times were grouped in the 50–500 ms range with a few isolated events of longer duration. At an applied voltage of +100 mV (Fig. 12 *b*), the most common event duration remained 100 ms, but the size of the 50–500 ms population decreased. Finally, at an applied potential of +200 mV (Fig. 12 *c*), the 50–500 ms population has di-

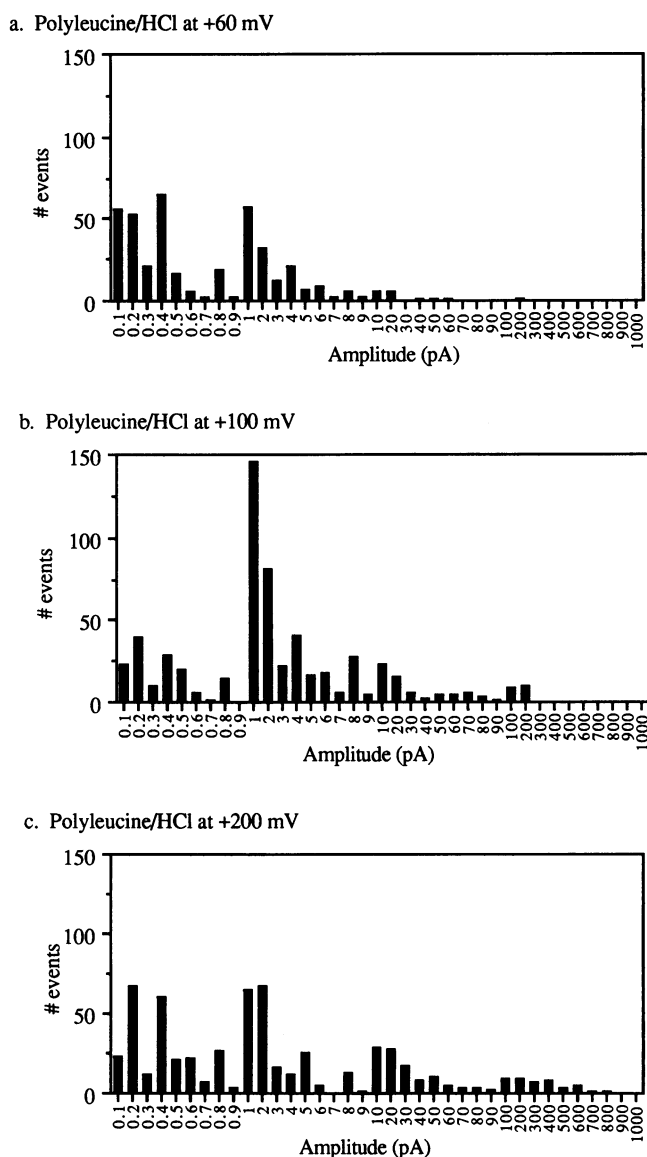


FIGURE 10 Amplitude histograms for polyleucine-induced defects in PE/PS (1:1) planar bilayers in 0.1 N HCl at the applied potential of (a) +60 mV, (b) +100 mV, and (c) +200 mV.

minished further, and the distribution of open times seemed to be shifted somewhat towards the longer-lived events.

## DISCUSSION

Maintaining ionic gradients is a primary function of biological membranes. If a cell membrane cannot provide an effective barrier to ion flux, cell dysfunction and death quickly follow. The lipid bilayer moiety of the membrane provides a low dielectric barrier to ionic flux, so that ion channels can be considered to be high dielectric pores across the nonpolar bilayer phase. One such pore is produced when the  $\alpha$ -helices of relatively hydrophobic transmembrane proteins are incorporated into the bilayer.

Bacteriorhodopsin was the first membrane protein shown to be composed of a single peptide strand forming seven

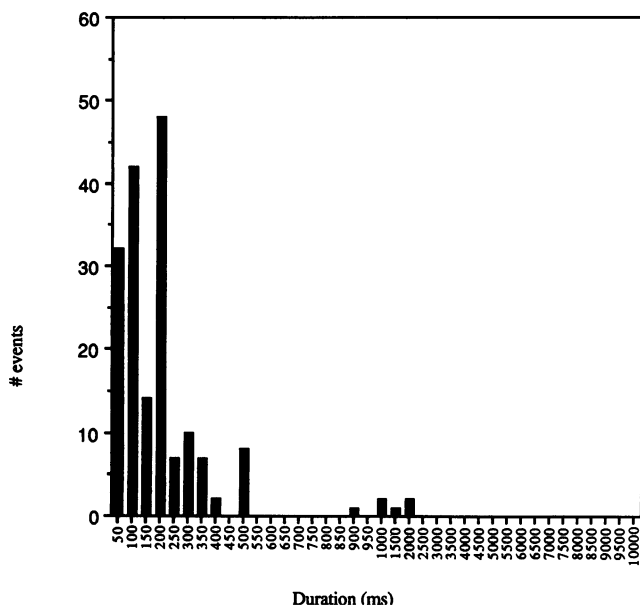


FIGURE 11 Open time duration histogram for long-chain polyaniline-induced defects in PE/PS (1:1) planar bilayers at +60 mV applied potential in 0.1 N HCl.

adjacent transmembrane  $\alpha$ -helices that outline a heptagonal bundle (Henderson and Unwin, 1975). Subsequently, multi-subunit bundles of  $\alpha$ -helices have been proposed for the transmembrane structures of several ionic channels and pumps, including the acetylcholine receptor (for review, see Guy and Hucho, 1987), the sodium channel (Caterall, 1986), the anion exchange band 3 protein of the red cell membrane (Jay and Cantley, 1986), and the  $\text{Na}^+/\text{K}^+$  ATPase (Ovchinnikov, 1987). The foundations for most of these structures were hydropathy plots (Kyte and Doolittle, 1982), which suggested probable transmembrane helical segments of the proteins.

Because very little is known about the packing properties of  $\alpha$ -helices or the interactions between helical bundles and ions, computer modeling has been used to investigate the conductive properties of  $\alpha$ -helical bundles in bilayers. Furois-Corbin and Pullman (1986a, b, 1987a, b) performed energy minimization studies, taking into account atom-atom interactions over all the atoms, and including all components of the interaction energy (electrostatic, Van der Waals-London, polarization, and torsion), for bundles of various length, polarity, and number of  $\alpha$ -helices. It was found that with helices of 14 residues or more, the Van der Waals-London component dominates the energy. Transmembrane helices must be at least 20 residues in length. Thus, although the electrostatic term favors antiparallel helices in a membrane, the presence of one pair of parallel helices in a helix bundle does not necessarily destabilize the bundle (for review, see Pullman, 1988). This would be analogous to folding a peptide through the bilayer an odd number of times as is the case with bacteriorhodopsin.

To examine the possibility that an ion passes through such model channels, energy profiles were constructed in which

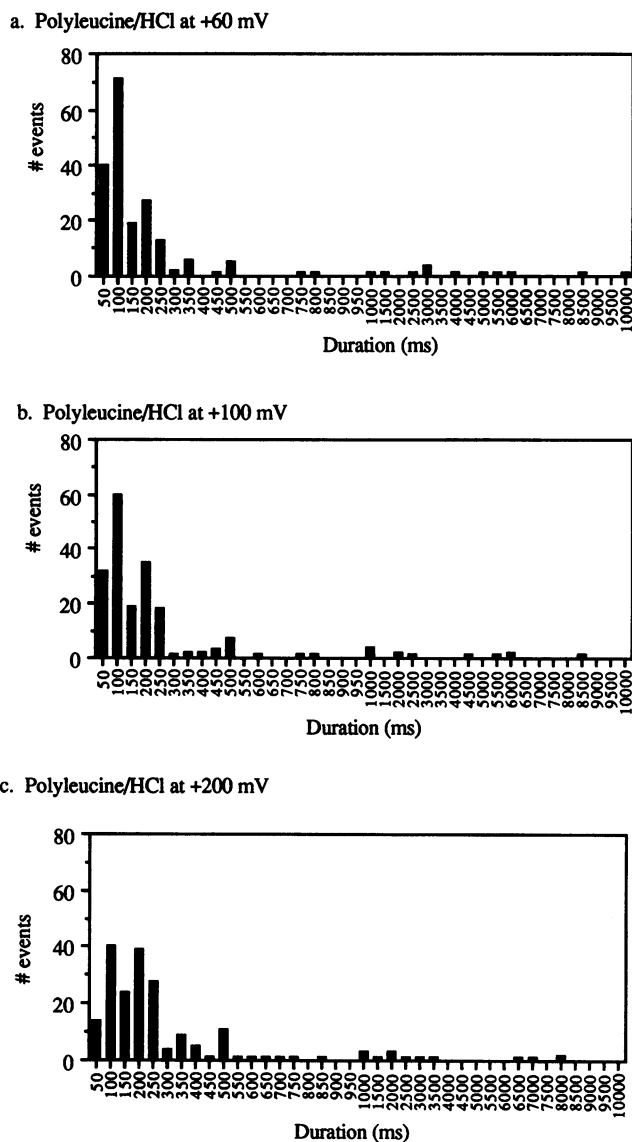


FIGURE 12 Open time duration histograms for polyleucine-induced defects in PE/PS (1:1) planar bilayers in 0.1 N HCl at the applied potential of (a) +60 mV, (b) +100 mV, and (c) +200 mV.

the total interaction energy between a  $\text{Na}^+$  ion and a five-helix bundle of poly-(L-alanine)<sub>14</sub> was plotted against the distance through the bilayer. Because the peptides were 14 residues in length, the helices spanned only 22 Å of the theoretical membrane. Energetic interactions between polyaniline helix pairs, however, were constant with peptides of 13 or more residues. Therefore, a length of 14 residues was chosen for the peptides in the helix bundle (Furois-Corbin and Pullman, 1986b).

The most significant finding is that at every axial level tested, the ion and the channel have a negative (favorable) interaction energy possible (Furois-Corbin, 1986b). Thus, it follows that neither charged nor uncharged polar residues are necessary in the lining of an ion channel for ion translocation to occur. The carbonyl oxygens of the peptide bonds may provide sufficient attraction to allow the ion to find a path through the channel (Pullman, 1988).

To test this concept, we incorporated a variety of poly-amino acids in lipid bilayers, examining both their effect on the permeation of protons and other ions across bilayer membranes of liposomes, and the nature of the conducting pathway with planar lipid membranes. We found that long-chain polyalanine and polyleucine caused substantial increases in proton permeability, whereas polyhistidine had little effect. The hydrophilic peptide polyhistidine, therefore, served as an internal control. Our results indicate that, using the liposome preparation method described, about one hundred of the long-chain hydrophobic polyamino acids were associated with each liposome. Moreover, FTIR spectroscopy showed that, in a lipid environment, 66% of the long-chain polyalanine and 79% of the polyleucine existed in an  $\alpha$ -helical conformation.

This result would follow from the observation of Brown and Huestis (1992) that even short hydrophobic peptides can insert deep into the lipid bilayer interior, with conformation influenced by the nonpolar environment. In a bilayer, where fatty acid hydrocarbon tails are the solvent, intermolecular hydrogen bonding is not possible, so that helical secondary structures that satisfy intramolecular backbone hydrogen bonds are the most energetically favorable (Wallace, 1988). In fact, the secondary structure of poly-L-alanine and poly-L-leucine has been shown by optical rotary dispersion to be almost entirely  $\alpha$ -helical in the nonpolar environment of  $\text{CHCl}_3$  (Fasman, 1962).

Computer modeling (Furois-Corbin and Pullman, 1986, 1987; for review, see Pullman, 1988) predicted that bundles of  $\alpha$ -helices composed of hydrophobic polyamino acids could conduct ions in the absence of any charged or polar residues. Our results indicate that long-chain hydrophobic polyamino acids can cause proton-conducting defects. Potassium-conducting defects, however, were not seen. This suggests that the ionic current can only be conducted along hydrogen-bonded chains of water, thereby providing high proton selectivity. The specific mechanism proposed by Furois-Corbin and Pullman (1986)—that ions can be translocated along carbonyl oxygens of peptide bonds—does not appear to be operating in the case of the poly-amino acid-induced defects reported here. This mechanism should be able to conduct sodium, potassium, and hydrogen ions, but the long-chain hydrophobic poly-amino acids produce membrane defects accessible only to protons.

One explanation for the lack of potassium conductance is that the transmembrane helices of polyalanine and polyleucine are unable to form stable bundles of sufficient size to admit potassium ions. A similar observation was reported earlier by Lear et al. (1988), who could demonstrate either proton selectivity or potassium selectivity with two different leucine-serine peptides. Computer models of the putative channels showed that tetrameric bundles might only accommodate proton flux, whereas pentamers and hexamers could accommodate larger hydrated cations.

## The influence of peptide length on ion conduction

In comparing the proton permeability effects caused by the 275-residue polyalanine and the 55-residue polyalanine, it became clear that peptides long enough to span the membrane several times were considerably more effective at proton conduction than peptides long enough to cross the membrane only twice. The effect is even greater, when we consider that less long-chain polyalanine was associated with the vesicles than short-chain polyalanine. This finding can be explained by looking at the relative probability of each type of peptide forming an ion-conducting bundle. For short-chain polyalanine, three or four individual molecules would need to form bundles in the bilayer with appropriate conformation and orientation. In the case of long-chain polyalanine, however, up to 10 membrane-spanning  $\alpha$ -helices may form from a single molecule. This linked arrangement increases the probability that several  $\alpha$ -helices will aggregate to form a bundle that spans the bilayer.

In addition,  $\alpha$ -helices spanning the membrane possess electric dipoles that attract each other if anti-parallel and repel each other if parallel (Edmonds, 1985). If the long-chain polyalanine spans the membrane several times, there is a higher probability that two nearest neighbor  $\alpha$ -helices would be anti-parallel than for short-chain polyalanine. Because the adjacent anti-parallel helices of long-chain polyalanine would tend to attract each other, this would also increase the likelihood of formation of an ion-conducting bundle.

These results correlate well with known membrane permeability effects caused by biological proteins. Glycophorin, which has a single membrane spanning domain, does not substantially increase vesicle permeability to  $\text{Na}^+$  or  $\text{Rb}^+$  even when incorporated by dialysis at high protein/lipid ratios (Mimms et al., 1981). A different result was obtained, however, when only the transmembrane hydrophobic domain of glycophorin was incorporated into vesicles, a form that can aggregate in the bilayer (Romans et al., 1981). At high peptide/lipid ratios,  $^{22}\text{Na}^+$  efflux from liposomes was biphasic. Increasing the peptide/lipid ratio had no effect on slow efflux, which was due to leakage around peptide monomers, but increased fast efflux, which was thought to be due to leakage through peptide multimers. Particles of 80 Å could be visualized with freeze-fracture electron microscopy, and provided additional evidence that peptide multimers were present in the bilayer (Romans et al., 1981).

Finally, many receptor-ionophore complexes, such as the acetylcholine receptor or the  $\gamma$ -amino butyric acid receptor, are composed of four or five linked subunits that surround an ion channel (Cooper et al., 1991; Kosower, 1987; for review, see Olsen and Tobin, 1990; Barnard et al., 1987).

## Hydrophobic peptides with amphipathic helices

An amphipathic helix is one in which polar residues are aligned vertically, parallel to the axis of the helix, and are found on only one side of the helical structure. Many pore

forming proteins, for example, alamethicin, the magainins, and other lytic peptides, form amphipathic helices in the membrane (for review, see Segrest et al., 1990). Synthetic amphipathic helices have also been constructed that clearly demonstrate ion conducting capabilities (Lear et al., 1988; Epand et al., 1989; Parente et al., 1990), and in one case, proton specificity (Lear et al., 1988). The many varied conductance states and types of ions conducted by these channels suggest that the polar residues along the channel of pore-forming amphipathic helices aid ion conduction.

The hydrophobic polyamino acids tested in this study, however, were efficient conductors only of protons. In addition, the polyamino acids were extremely difficult to incorporate into the liposome membrane. A heated incubation of a polyamino acid/lipid film was required to allow polyamino acid incorporation into the bilayer. The amphipathic alamethicin, on the other hand, could be added externally to pre-formed liposomes and spontaneously entered the bilayer. It has been found that the membrane surface can act as an interface between the external aqueous solution and the hydrophobic membrane core. Amphipathic helix, which is partially embedded in a membrane (i.e., along its nonpolar surface) is likely to insert into the bilayer interior due to a favorable free energy gradient (Jacobs and White, 1989). Therefore, although it is possible for chains of entirely hydrophobic polyamino acids to cause ion-conducting defects in a lipid bilayer, complex amino acid sequences are likely to have evolved due to advantage in insertion, selectivity, and conductance.

### Liposome permeability results are supported by planar bilayer data

The two strongest points of similarity between the results of the liposomal membrane permeability investigation and those obtained from planar bilayer recordings are that (a) long-chain polyalanine and polyleucine produced the largest effect of any polyamino acids studied on membrane permeability and ionic conductance, and (b) those parameters were significantly affected only in the case of protons. Current fluctuations produced by polyamino acids in planar bilayers have been reported previously. Heitz et al. (1982), for instance, described conductive events lasting up to a few seconds that were caused by poly-L-alanine in glyceryl monooleate or dioleoylphosphatidylcholine bilayers. Poly-D, L-proline has also been shown to be capable of causing channel-like events in glyceryl monooleate membranes (De Santis et al., 1985). To our knowledge, however, the present study is the first attempt to correlate the findings of liposome permeability to results obtained with single channel recording from planar lipid bilayers.

A correlation between the results from the two techniques can also be demonstrated by calculating whether the polyleucine-induced conductive defects can account for the increased proton permeability seen in polyleucine liposomes. For this purpose, we took the volume of a 0.2- $\mu\text{m}$  liposome to be  $4 \times 10^{-18}$  l, and the measured buffer capacity of the

AMTT buffer was 9 mM per pH unit, with good linearity in the experimental range from pH 6 to 8. From this, it is readily calculated that approximately 22,000 protons must enter a single liposome to discharge a pH gradient of 1 unit in 10 mM AMTT near pH 7.

For polyleucine-induced defects in planar bilayers (pH 1) at +60 mV applied potential (which corresponds to a 1 pH unit proton gradient), the mean current through an open defect is 3.4 pA, or  $3.5 \times 10^{-17}$  mol  $\text{H}^+$ /s. Assuming a linear relationship between proton concentration and ionic current extrapolated from pH 1 to 7 (the pH range for the liposome experiments), the number of protons moving through an open defect at pH 7 would be 21 protons  $\text{s}^{-1}$ .

The mean number of polyleucine molecules per liposome is 135. If we assume that all the peptides formed open defects, the rate of protons moving into the liposome would be 2,835  $\text{H}^+ \text{s}^{-1}$  liposome $^{-1}$ , so that 8 s would be required for 22,500 protons to cross the bilayer and deplete a 1-pH-unit gradient. For polyalanine, the same calculation suggests that 2.2 min would be required to deplete the proton gradient across the liposomal membrane. Given the uncertainties of such calculations and extrapolations, and considering that only a fraction of the peptide-induced channels would be open at any given time, these values are in reasonable agreement with measured decay times of buffered pH gradients, which have half-times of minutes.

### A possible conduction mechanism and relationship to proton translocation in biomembranes

We found that hydrophobic peptides are able to conduct protons but not potassium ions. For instance, in planar membranes containing polyleucine, conductive events in the range of tens to hundreds of picoamps were observed in HCl at 200 mV, whereas essentially no events were seen in KCl at the same voltage. This result suggests that the proton/potassium selectivity is at least 100 in polyleucine channels. To explain the proton selectivity, we propose that the conduction events involve transient hydrogen-bonded chains (tHBCs) of water (for reviews, see Nagle and Tristram-Nagle, 1983; Deamer, 1987; Deamer and Nichols, 1989). This mechanism would not transport potassium ions, which can only be translocated by classic diffusion. If the defect caused by the hydrophobic polyamino acids was not organized enough to be a true "channel," it might at least be able to provide an environment favorable to the ordering of water molecules in the membrane, thereby permitting transient hydrogen-bonded chains of water to form.

The most convincing example of transmembrane proton conduction along hydrogen-bonded chains of water is gramicidin. Gramicidin is a 15-residue peptide with alternating D- and L-hydrophobic amino acids (Sarges and Witkop, 1964). Each peptide forms a  $\beta$ -helix in the membrane with a 0.4 nm central pore. Ion channels are formed when two molecules join head-to-head in a hydrogen-bonded dimer to span the bilayer (Tosteson et al., 1968; Goodall, 1971; for review, see

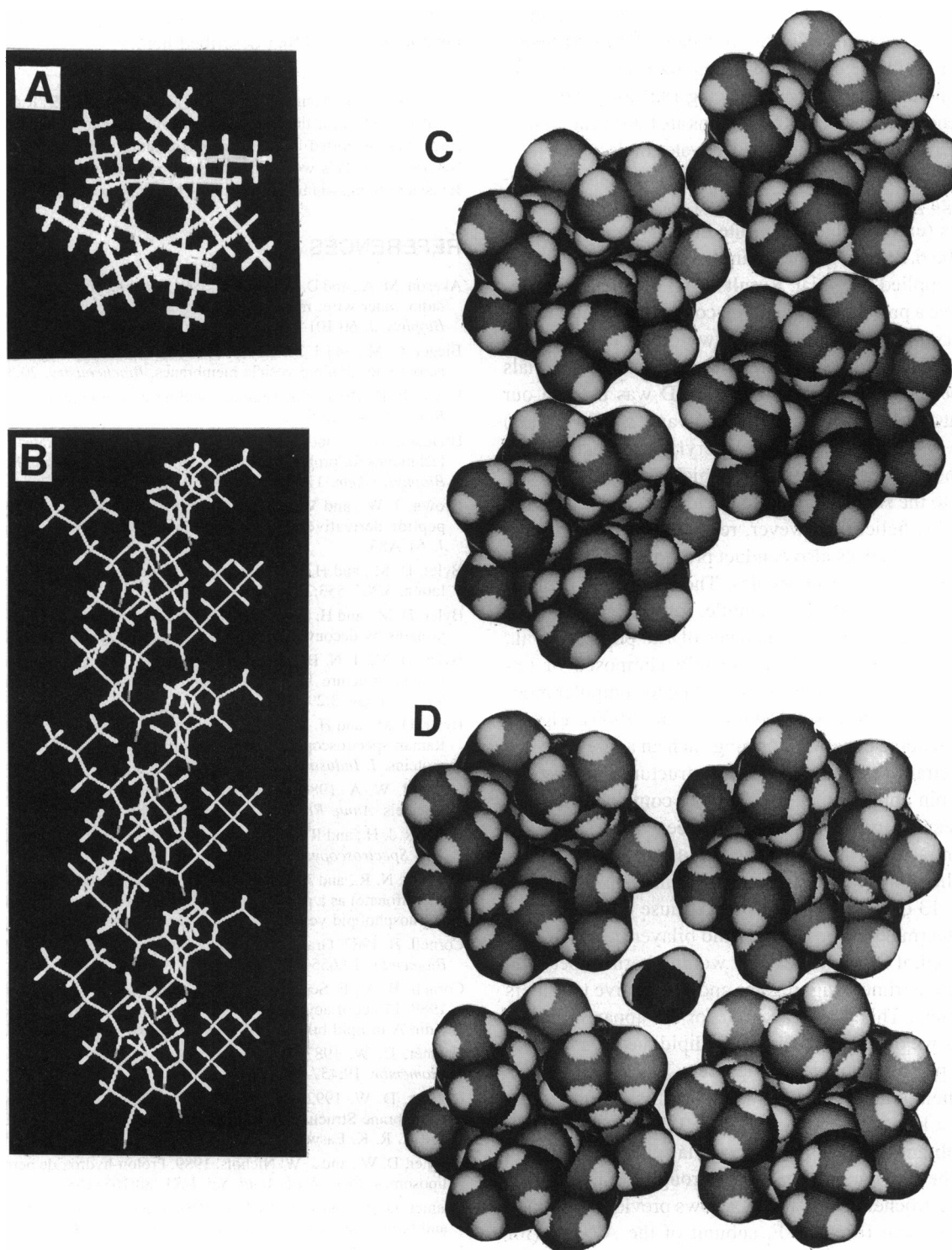


FIGURE 13 Computer-generated  $\alpha$ -helical aggregates. Polyleucine  $\alpha$ -helices (20 residues) were produced with MacIcmdad software (Molecular Applications Group, Stanford University, Stanford CA). The backbone structure is shown from above in 13 A, and in side view in 13 B. CPK space-filling versions of the top view were then fitted to show the 3a structure (13 C), described by Furois-Corbin and Pullman (1986), which excludes water, and the 4a structure (13 D), which may include a chain of water molecules. Certain pentameric aggregates (not shown) have ample room to provide an aqueous channel. The bundles of  $\alpha$ -helices shown here are for illustration only. No attempt was made to find energy-optimized structures.

Cornell, 1987). The gramicidin channel conducts protons at an anomalously high rate compared to  $K^+$  and  $Na^+$  ions (Myers and Haydon, 1972; Akeson and Deamer, 1991). Protons were shown to be conducted along water wires through

gramicidin by Levitt (1978), who demonstrated that conduction of other cations through gramicidin produced streaming potentials across the membrane, but that proton conduction did not have this effect. Streaming potentials are

caused when nonhydrogen cations move through the pore in single file, forcing a line of water molecules to move as well. Protons, in contrast, can move along transient hydrogen-bonded chains of water without producing a streaming potential. It is now generally considered that protons are translocated along a strand of 10 to 12 hydrogen-bonded water molecules.

Hladky and Haydon (1972) found the conductance of protons through gramicidin A channels in glyceryl monooleate membranes (extrapolated to infinite dilution in aqueous solution) to be 6.1 times greater than that of potassium ions at +100 mV applied potential. Results from the present investigation gave a proton/potassium ion conductance ratio of 3.1 at +100 mV applied potential. The twofold discrepancy between these findings may be due to the use of different materials in the experimental set-up. Gramicidin D was used in our experiments, instead of gramicidin A, and a PE/PS (1:1) membrane was used instead of glyceryl monooleate.

The  $\beta$ -helix structure of the gramicidin channel is not analogous to the structure of a typical ion channel composed of clustered  $\alpha$ -helices. However, recent work suggests that aggregates of  $\alpha$ -helices also conduct protons along chains of hydrogen-bonded water molecules. The 21-residue peptide,  $H_2N$ -(L<sub>1</sub>S<sub>2</sub>L<sub>3</sub>L<sub>4</sub>L<sub>5</sub>L<sub>6</sub>)<sub>3</sub>-CONH<sub>2</sub>, for example, forms highly proton-selective channels with a conductance of 120 pS (Lear et al., 1988). The proton channel is probably composed of tetrameric aggregates of  $\alpha$ -helices, according to computer modeling work (for review, see DeGrado et al., 1989). Fig. 13 shows polyleucine  $\alpha$ -helices forming such an aggregate. It is clear that tetramers bundled in the 4a structure proposed by Furois-Corbin and Pullman (1986) may contain a chain of water molecules in the interstices between helices (Fig. 13 D). In contrast, as noted by these authors, more tightly packed helices would be unable to accommodate interstitial water (Fig. 13 C). We also note that because the helices are subject to thermal motions of the fluid bilayer in which they are embedded, it is likely that they would alternate between nonconductive trimeric aggregates and conductive tetramers and pentamers. This would account for the apparent gating phenomena we observed in the planar lipid membranes with associated polyalanine and polyleucine.

A transmembrane enzyme complex in which proton translocation is a key function is the  $F_1F_0$  ATP synthase of coupling membranes such as mitochondria, chloroplasts, and bacteria. The movement of protons through the  $F_0$  subunit, down an electrochemical gradient, allows previously formed ATP to dissociate from the  $F_1$  subunit of the ATPase (for review, see Boyer, 1988). It has been suggested that protons may move through the  $F_0$  subunit along hydrogen-bonded chains of water molecules (Hoppe and Sebald, 1984; Akeson and Deamer, 1991). This idea has been investigated using gramicidin as a model, and it was found that a water wire would be kinetically competent to support the level of proton conductance through  $F_0$  necessary in the production of ATP (Akeson and Deamer, 1991). Direct evidence that the  $F_0$  channel uses this mechanism for proton transport has not yet been established, but it is clearly possible that tetrameric bundles of  $\alpha$ -helices may exist at the interfaces between the a and c subunits

of the ATPase  $F_0$  complex and provide a proton-conducting channel similar to that described here.

We wish to express our appreciation to Mr. John Mais, Mr. Rick Harris, and Dr. Allen Gibbs for their expert technical instruction and assistance. This study was supported by National Aeronautics and Space Administration NAGW-1119. This work was presented in a preliminary form at the 25<sup>th</sup> Jerusalem Symposium on Quantum Chemistry and Biochemistry, 1992.

## REFERENCES

- Akeson, M. A., and D. W. Deamer. 1991. Proton conductance by the gramicidin water wire: model for proton conductance in the  $F_1F_0$  ATPases? *Biophys. J.* 60:101-109.
- Biegel, C. M., and J. M. Gould. 1981. Kinetics of hydrogen ion diffusion across phospholipid vesicle membranes. *Biochemistry.* 20:3474-3479.
- Boyer, P. D. 1988. Bioenergetic coupling to proton motive force. *Trends Biochem. Sci.* 13:5-7.
- Braiman, M. S., and K. J. Rothschild. 1988. Fourier transform infrared techniques for probing membrane protein structure. *Annu. Rev. Biophys. Chem.* 17:541-570.
- Brown, J. W., and W. H. Huestis. 1992. Interactions of a hydrophobic peptide derivative with unilamellar phospholipid vesicles. *Biophys. J.* 61:A83.
- Byler, D. M., and H. Susi. 1985. Protein structure by FTIR self-deconvolution. *SPIE.* 553:289-290.
- Byler, D. M., and H. Susi. 1986. Examination of the secondary structure of proteins by deconvolved FTIR spectra. *Biopolymers.* 25:469-487.
- Byler, D. M., J. N. Brouillette, and H. Susi. 1986. Quantitative studies of protein structure by FTIR spectral deconvolution and curve fitting. *Spectroscopy.* 3:29-32.
- Byler, D. M., and H. Susi. 1988. Application of computerized infrared and Raman spectroscopy to conformation studies of casein and other food proteins. *J. Industrial Microbiol.* 3:73-88.
- Catterall, W. A. 1986. Molecular properties of voltage-sensitive sodium channels. *Annu. Rev. Biochem.* 55:953-985.
- Clark, R. J. H., and R. E. Lester. 1986. Spectroscopy of biological systems. *Adv. Spectroscopy.* 13:1-46.
- Clement, N. R., and J. M. Gould. 1981. Pyranine (8-hydroxy-1,3,6-pyrenetrisulfonate) as a probe of internal aqueous hydrogen ion concentration in phospholipid vesicles. *Biochemistry.* 20:1534-1538.
- Cornell, B. 1987. Gramicidin A-phospholipid model systems. *J. Bioenerg. Biomembr.* 19:655-676.
- Cornell, B. A., F. Separovic, D. E. Thomas, A. R. Atkins, and R. Smith. 1989. Effect of acyl chain length on the structure and motion of gramicidin A in lipid bilayers. *Biochim. Biophys. Acta.* 985:229-232.
- Deamer, D. W. 1987. Proton permeation of lipid bilayers. *J. Bioenerg. Biomembr.* 19:457-479.
- Deamer, D. W. 1992. Role of water in proton flux mechanisms. In *Biomembrane Structure and Function—The State of the Art.* B. P. Gaber and K. R. K. Easwaran, editors. Adenine Press, New York. 209-224.
- Deamer, D. W., and J. W. Nichols. 1989. Proton-hydroxide permeability of liposomes. *Proc. Natl. Acad. Sci. USA.* 80:165-168.
- Deamer, D. W., and J. W. Nichols. 1989. Proton flux mechanisms in model and biological membranes. *J. Membr. Biol.* 107:91-103.
- De Grado, W. F., Z. R. Wasserman, and J. D. Lear. 1989. Protein design, a minimalist approach. *Science.* 243:622-628.
- De Santis, P., A. Palleschi, M. Savino, A. Scipioni, B. Sesta, and A. Verdini. 1985. Poly-D, L-Proline, a synthetic polypeptide behaving as an ion channel across bilayer membranes. *Biophys. Chem.* 21:211-215.
- Edmonds, D. T. 1985. The  $\alpha$ -helix dipole in membranes: a new gating mechanism for ion channels. *Eur. Biophys. J.* 13:31-35.
- Eisenberg, M., J. E. Hall, and C. A. Mead. 1973. The nature of the voltage-dependent conductance induced by alamethicin in black lipid membranes. *J. Membr. Biol.* 14:143-176.
- Epand, R. M., W. K. Surewicz, D. W. Hughes, H. Mantsch, J. P. Segrest, T. M. Allen, and G. M. Anantharamaiah. 1989. Properties of lipid complexes with amphipathic helix-forming peptides. *J. Biol. Chem.* 264:4628-4635.

- Ernster, L., and G. Schatz. 1981. Mitochondria: a historical review. *J. Cell Biol.* 91:227S–255S.
- Fasman, G. D. 1962. The relative stabilities of the  $\alpha$ -helix in synthetic polypeptides. In *Polyamino Acids, Polypeptides, and Proteins*. M. Stahmann, editor. University of Wisconsin Press, Madison, WI. 221–228.
- Fillingame, R. H. 1980. The proton-translocating pumps of oxidative phosphorylation. *Annu. Rev. Biochem.* 49:1079–1113.
- Furois-Corbin, S., and A. Pullman. 1986a. Theoretical study of the packing of  $\alpha$ -helices by energy minimization: effect of the length of the helices on the packing energy and on the optimal configuration of a pair. *Chem. Phys. Lett.* 123:305–310.
- Furois-Corbin, S., and A. Pullman. 1986b. Theoretical study of the packing of  $\alpha$ -helices of poly ( $\alpha$ -alanine) into transmembrane bundles. Possible significance for ion transfer. *Biochim. Biophys. Acta.* 860:165–177.
- Furois-Corbin, S., and A. Pullman. 1987a. Theoretical study of potential ion channels formed by a bundle of  $\alpha$ -helices: effect of the presence of polar residues along the channel inner wall. *J. Biomol. Struct. Dyn.* 4:589–598.
- Furois-Corbin, S., and A. Pullman. 1987b. Theoretical study of the packing of  $\alpha$ -helices into possible transmembrane bundles. Sequences including alanines, leucines, and serines. *Biochim. Biophys. Acta.* 902:31–45.
- Goodall, M. C. 1971. Thickness dependence in the action of gramicidin A on lipid bilayers. *Arch. Biochem. Biophys.* 147:129–135.
- Guy, H. R., and F. Hucho. 1987. The ion channel of the nicotinic acetylcholine receptor. *Trends Neurosci.* 10:318–321.
- Hall, J. E., I. Vodyanoy, T. M. Balasubramanian, and G. R. Marshall. 1984. Alamethicin, a rich model for channel behavior. *Biophys. J.* 45:233–247.
- Hausser, H., D. Oldani, and M. C. Phillips. 1973. Mechanism of ion escape from phosphatidylcholine and phosphatidylserine single bilayer vesicles. *Biochemistry.* 12:4507–4517.
- Heitz, F., G. Spach, P. Seta, and C. Gavach. 1982. Ion conducting pores induced by oligo-L-alanine. *Biochem. Biophys. Res. Commun.* 107:481–484.
- Henderson, R., and P. T. N. Unwin. 1975. Three-dimensional model of purple membrane obtained by electron microscopy. *Nature.* 257:28–32.
- Hladky, S. B., and D. A. Haydon. 1972. Ion transfer across lipid membranes in the presence of gramicidin A. *Biochim. Biophys. Acta.* 274:294–312.
- Hoppe, J., and W. Sebald. 1984. The proton-conducting  $F_0$  part of bacterial ATP synthases. *Biochim. Biophys. Acta.* 768:1–27.
- Jacobs, R. E., and S. H. White. 1989. The nature of the hydrophobic binding of small peptides at the bilayer interface: implications for the insertion of transbilayer helices. *Biochemistry.* 28:3421–3437.
- Jay, D., and L. Cantley. 1986. Structural aspects of the red cell anion exchange protein. *Ann. Rev. Biochem.* 55:511–538.
- Kano, K., and J. H. Fendler. 1978. Pyranine as a sensitive pH probe for liposome interiors and surfaces. *Biochim. Biophys. Acta.* 509:289–299.
- Krimm, S. 1962. Infrared spectra and chain conformation of proteins. *J. Mol. Biol.* 4:528–540.
- Kyte, J., and R. F. Doolittle. 1982. A simple method for displaying the hydrophobic character of a protein. *J. Mol. Biol.* 157:105–132.
- Lear, J. D., Z. R. Wasserman, and W. F. De Grado. 1988. Synthetic amphiphilic peptide models for protein ion channels. *Science.* 240:1177–1181.
- Levitt, D. G., S. R. Elias, and J. M. Hautman. 1978. Number of water molecules coupled to the transport of sodium, potassium and hydrogen ions via gramicidin, nonactin or valinomycin. *Biochim. Biophys. Acta.* 512:436–451.
- Mimms, L. T., G. Zampighi, Y. Nozaki, C. Tanford, and A. Reynolds. 1981. Phospholipid vesicle formation and transmembrane protein incorporation using octyl glucoside. *Biochemistry.* 20:833–840.
- Myers, V. B., and D. A. Haydon. 1972. Ion transfer across lipid membranes in the presence of gramicidin A. *Biochim. Biophys. Acta.* 274:313–322.
- Nagle, J. F., and S. T. Tristram-Nagle. 1983. Hydrogen-bonded chain mechanisms for proton conduction and proton pumping. *J. Membr. Biol.* 74:1–14.
- Nichols, J. W., and D. W. Deamer. 1980. Net proton-hydroxyl permeability of large unilamellar liposomes measured by an acid-base titration technique. *Proc. Natl. Acad. Sci. USA.* 77:2038–2042.
- Ovchinnikov, Y. A. 1987. Membrane protein functioning. In *Ion Transport Through Membranes*. K. Yagi and B. Pullman, editors. Academic Press, New York. 61–83.
- Papa, S. 1982. Molecular mechanism of proton translocation by the cytochrome system and the ATPase of mitochondria. Role of proteins. *J. Bioenerg. Biomembr.* 14:69–86.
- Parente, R. A., L. Nadasdi, N. K. Subbarao, and F. C. Szoka, Jr. 1990. Association of a pH-sensitive peptide with membrane vesicles: role of amino acid sequence. *Biochemistry.* 29:8713–8719.
- Pennington, R. M., and R. R. Fisher. 1981. Dicyclohexyl-carbodiimide modification of bovine heart mitochondrial transhydrogenase. *J. Biol. Chem.* 256:8963–8969.
- Perkins, W. R., and D. S. Cafiso. 1986. An electrical and structural characterization of  $H^+$ / $OH^-$  currents in phospholipid vesicles. *Biochemistry.* 25:2270–2276.
- Portlock, S. H., M. J. Clague, and R. J. Cherry. 1990. Leakage of internal markers from erythrocytes and lipid vesicles induced by melittin, gramicidin S, and alamethicin: a comparative study. *Biochim. Biophys. Acta.* 1030:1–10.
- Pullman, A. 1988. Theoretical studies on the formation and properties of bundles of  $\alpha$ -helices and their aptitude to form ion channels. *Prog. Clin. Biol. Res.* 273:113–120.
- Romans, A. Y., T. M. Allen, W. Meckes, R. Chiovetto Jr., L. Sheng, H. Decret, and P. Segrest. 1981. Incorporation of the transmembrane hydrophobic domain of glycophorin into small unilamellar phospholipid vesicles. Ion flux studies. *Biochim. Biophys. Acta.* 642:135–148.
- Sarges, R., and B. Witkop. 1964. Gramicidin A IV. Primary sequence of valine and isoleucine Gramicidin A. *J. Am. Chem. Soc.* 86:1862–1863.
- Segrest, J. P., H. DeLoof, J. G. Dohlman, C. G. Brouillette, and G. M. Anatharamaiah. 1990. Amphipathic helix motif: classes and properties. *Proteins Struct. Funct. Genet.* 8:103–117.
- Smith, R., D. E. Thomas, F. Separovic, A. R. Atkins, and B. Cornell. 1989. Determination of the structure of a membrane-incorporated ion channel. Solid state nuclear magnetic resonance studies of gramicidin A. *Biophys. J.* 56:307–314.
- Stoeckenius, W., R. H. Lozier, and R. A. Bogomolni. 1979. Bacteriorhodopsin and the purple membrane of halobacteria. *Biochim. Biophys. Acta.* 505:215–278.
- Susi, H., and D. M. Byler. 1983. Protein structure by Fourier transform infrared spectroscopy second derivative spectra. *Biochem. Biophys. Res. Commun.* 115:391–397.
- Susi, H., and D. M. Byler. 1983. Protein structure by FTIR spectroscopy second derivative spectra. *Biochem. Biophys. Res. Commun.* 115:391–397.
- Tosteson, D. C., T. E. Andreoli, M. Tieffenberg, and P. Cook. 1968. The effects of macrocyclic compounds on cation transport in sheep red cells and thin and thick lipid membranes. *J. Gen. Physiol.* 51:373S–384S.
- Wallace, B. A. 1988. Membrane protein folding: motifs and predictions. *Prog. Clin. Biol. Res.* 273:133–138.
- Wikstrom, M., K. Krab, and M. Saraste. 1981. Proton-translocating cytochrome complexes. *Annu. Rev. Biochem.* 50:623–655.
- Urry, D. W. 1971. The gramicidin A transmembrane channel: a proposed  $\pi_{(L,D)}$  Helix. *Proc. Natl. Acad. Sci. USA.* 68:672–678.